International Journal on Engineering Technologies and Informatics

Ground-Motion Predictions for California: Comparisons of Three GMPEs

Research Article

Volume 3 Issue 2- 2022

Author Details

Erol Kalkan and Vladimir Graizer*

Department of Civil and Environmental Engineering, University of California Davis, USA

*Corresponding author

Erol Kalkan, Department of Civil and Environmental Engineering, University of California Davis, Davis, CA 95616, USA

Article History

Received: July 12, 2022 Accepted: : August 09, 2022 Published: August 16, 2022

Abstract

We systematically evaluate data sets, functional forms, independent parameters of estimation and resulting ground motion predictions (as median and aleatory variability) of the Graizer-Kalkan [1,2] ground motion prediction equation (GMPE) with the next generation of attenuation project (NGA-West2) models of Abrahamson et al. [3] and Boore et al. [4] for application to earthquakes in California. This evaluation is performed in three stages: (1) by comparing attenuation, magnitude scaling, style-of-faulting (SOF) effects, site response, response-spectral shape and amplitude, and standard deviations, (2) by comparing median predictions, standard deviations and analyses of residuals with respect to near-field (within 20 km of the fault) and intermediate-field (50 to 70 km of the fault) records from major earthquakes in California, and (3) by comparing total, intra- and inter-event residual distributions among the GMPEs with respect to near-source—within 80 km of the fault—subset of the NGA-West2 database covering 975 ground motions from 73 events in California ranging from moment magnitude 5 to 7.36. The results reveal that the scaling features of the GK15 and the ASK14 and BSSA14 GMPEs are, in general, similar in terms of distance attenuation but differ in terms of scaling with magnitude, style of faulting and site effects. The original standard deviations of GMPEs are also different. For the near-source California subset, three GMPEs result in standard deviations close to each other. The mixed-effect residuals analysis shows that the GK15 has no perceptible trend with respect to the independent predictors.

Introduction

The previous version of the Graizer-Kalkan ground-motion prediction equation (GMPE) was developed using the NGA-West1 database [5] along with additional records from major events in California and a number of earthquakes from other shallow crustal continental regions [6,7]. The NGA-West2 project [8] and recent earthquake data [9] accentuated a need to include regionalization in GMPE to account for differences in far-source (beyond 80 km) distance attenuation and soil response. Motivated by this need, we have updated our GMPE to include a new anelastic attenuation term as a function of quality factor (Q0) to capture regional differences in far-source attenuation and a new frequency-dependent sedimentary-basin scaling term as a function of depth to the 1.5 km/s shear-wave velocity isosurface to improve ground-motion predictions for sites on deep sedimentary basins (GK15 does not explicitly consider strong basin amplification on shallow basins).

In this paper, we systematically compare the data sets, functional forms, independent predictor variables and the resulting ground motion estimates (as median and aleatory variability) of GK15 with broadly used next generation of attenuation project (NGA-West2) models of Abrahamson et al. [3] and Boore et al. [10] for application to earthquakes in California. We do not include other three NGA-West2 models [11-13] for brevity and because they compare well with the ASK14 and BSSA14 [14]. The evaluation of the GMPEs here is performed in three stages:

1. compare distance attenuation, magnitude scaling, style-of-faulting (SOF) effects, site response, response-spectral shape and amplitude, and standard deviations,
2. compare median predictions, standard deviations and analyses of total residuals with respect to near-field (within 20 km of the fault) and intermediate-field (50 to 70 km of the fault) records from major earthquakes in California, and
3. compare total, intra- and inter-event residuals among the GMPEs by using a near-source—within 80 km of the fault [15]—subset of the NGA-West2 database.

©2022 Kalkan. This work is published and licensed by Example Press Limited. The full terms of this license are available at https://skeenapublishers.com/terms-conditions and incorporate the Creative Commons Attribution – Non Commercial (unported, v3.0) License (http://creativecommons.org/licenses/by-nc/3.0/). By accessing the work you hereby accept the Terms. Non-commercial uses of the work are permitted without any further permission from Emample Press, provided the work is properly attributed.

Data Set and Model Applicability Range

In development of the GK15, a total of 2,583 ground-motion recordings from 47 shallow crustal continental earthquakes with focal depths less than 20 km were used. This dataset, summarized in Table 1 in Kalkan and Graizer [16], includes events gathered from the Pacific Earthquake Engineering Research Center database created under the NGA-West1 project [5] and data from a number of additional events and stations. Approximately 70% of earthquakes are from California. This dataset, representing main shocks only, includes data recorded within 0.2 to 250 km of the earthquake faults from events in the magnitude range of 4.9 to 7.9. GMRotI50 is the intensity measure used in the development of NGA-West1 database [4]. See Kalkan et al. [16] for additional details.

NGA-West2 database (using GMRotD50) include 21,336 recordings from 600 shallow crustal earthquakes in the magnitude range of 3 to 7.9 and a rupture distance range of 0.05 to 1,533 km [17]. For ASK14, 15,750 recordings from 326 earthquakes were used in analyses for peak ground acceleration (PGA); among them 274 earthquakes with 12,044 recordings are from California. For BSSA14, 18,436 recordings from 404 events were utilized for PGA analyses. We did not use the NGA-West2 database for GK15 because it was not available to us.

Based on the final selected data sets used for GK15, ASK14 and BSSA14, the models' applicable range (in terms of magnitude, distance, VS30 and spectral periods) are listed in Table 2. Additional details are provided in individual papers describing these GMPEs. It should be also noted that GK15 provides the predictions for GMRotI50, a component definition different from that of the NGA-West2 models. We ignored the difference in definitions of component combination since it may be small and does not affect the results of comparisons [18-20].

Functional Forms and Parameters of GMPEs

The functional forms of ASK14 and BSSA14 GMPEs are significantly different than those of GK15. The ASK14 and BSSA14 GMPEs consist of single predictive equation covering both PGA and spectral acceleration (SA), however the GK15 is composed of two separate predictive equations. The first equation predicts PGA and the second equation constructs the spectral shape. The term spectral shape refers to the SA response spectrum normalized by PGA. The final SA response spectrum is obtained by anchoring the spectral shape to the PGA. In this model, the SA response spectrum is a continuous function of the spectral period, which is explained in details in Graizer et al. [7]. On the other hand, ASK14 and BSSA14 GMPEs use a discrete functional form for predicting the response spectral ordinates. The concept of a continuous function assumes cross-correlation of spectral ordinates at different periods [21] and de facto eliminates the difference between period intervals by making period intervals infinitesimally short. As a result, spectral ordinates are estimated smoothly and a long list of estimator coefficients for a range of spectral periods is eliminated [7].

Although ground motion distance attenuation is a complex process, in our opinion, its modeling should not require very complex models. We would like to explain our point of view by using the principle of parsimony, which argues that given a set of possible explanations, the simplest and competing explanation is the most likely to be correct [22]. In our case, the simplicity refers to the striking of a balance between consistency of a ground-motion prediction model with the observed earthquake data and the prior degree of belief in a model [23]. According to Jeffreys [24], the prior degree of belief in a model should be inversely related to the number of parameters. In GK15, simplicity postulates. This is evident in two ways. First, GK15 has only 31 estimator coefficients as compared to 1,008 estimator coefficients used in ASK14 and 2,889 coefficients used in BSSA14. Second, GK15 has a much simpler mathematical form than the other two GMPEs. In their book chapter, Vandekerckhove et al. [25] states that "goodness-of-fit must be balanced against model complexity to avoid overfitting—that is, to avoid building models that well explain the data at hand, but fail in out-of-sample predictions. The principle of parsimony forces researchers to abandon complex models that are tweaked to the observed data in favor of simpler models that can generalize to new data sets". To prevent overfitting, we not only avoided complex functions but also stopped adding new parameters when we had a high degree of belief that the residual errors are random rather than containing any further structure. We performed a detailed mixed-effects residual analysis to demonstrate that our simpler functional form and limited number of estimation coefficients were sufficient enough to reach unbiased ground motion estimates [1].

We present summary of independent parameters of estimations for the three GMPEs in Table 2. The distance metric for the GK15 and ASK14 is the closest distance to the rupture plane, Rrup. The BSSA14 uses the closest distance to the horizontal projection of the rupture plane, RJB. ASK14 also uses RJB for their hanging-wall function.

Each GMPE comprises a SOF parameter per their own faulting mechanism classification. The SOF parameter is dependent on magnitude for ASK14, whereas the SOF parameter of BSSA14 is magnitude independent. In GK15, the SOF parameter is adapted from Sadigh et al. [26], which is also magnitude independent. ASK14 contains an explicit functional form for hanging-wall sites and a rupture depth term. The BSSA14 indirectly accounts for hanging-wall features through the use of RJB without incorporating a rupture depth term and locations over fault plane have constant ground-motion values [27]. GK15 does not include a function form for hanging wall effect.

All three GMPEs are defined for a range in VS30 values (see Table 2). In ASK14, numerical simulations of nonlinear site amplification factors by Kamai et al. [27] were used for constraining the site response. In BSSA14, a semi-empirical nonlinear site response model by Seyhan et al. [28] was used; this model is based on empirical data and simulations of Kamai et al. [27]. For a reference site condition, the nonlinear site amplification factor is a function of PGA for BSSA14 and the SA for ASK14. The GK15 contains a linear site amplification feature based on the more limiting VS30 range. In addition to the VS30, ASK14 and BSSA14 also incorporate a parameter that is dependent on the depth to the 1.0 km/s shear-wave iso-surface (Z1.0) and the GK15 uses the depth to the 1.5 km/s shear-wave iso-surface (Z1.5). These extra parameters are to capture the difference in site amplification due to deep sedimentary basins. Furthermore, ASK14 uses the depth to the top of rupture (ZTOR), whereas GK15 and BSSA14 found depth parameter to be insignificant for ground-motion prediction with their mathematical form.

The NGA-West2 project [8] and recent earthquake data (e.g., [9] signify regionalization when accounting for differences in far-source distance attenuation of ground motions and site response. Hence, ASK14 and BSSA14 have developed regional adjustments for either site response and/or the long-distance anelastic attenuation between various geographical regions. BSSA14 incorporated only the regional attenuation adjustment feature. GK15 uses Q0¬—determined using Lg or coda waves—as an independent predictor that can be changed to suit the region of interest.

Stage 1: Comparisons of median predictions

3.3.1. Distance-scaling features: Figure 1a and Figure 2a compare the distance scaling features of the median estimates of PGA and SA at 0.2, 1.0 and 3.0 s for horizontal ground motions predicted by the three GMPEs for vertically dipping strike-slip earthquake scenarios with M5, 6, 7 and 8 as a function of Rrup for ASK14 and GK15, and as a function of RJB for BSSA14. Note that Rrup and RJB are same for vertical strike-slip events with the depth to top of the rupture equal to

zero (we did not include a comparison for dip-slip faults for brevity). The results are for National Earthquake Hazard Reduction Program (NEHRP) B/C reference site conditions (VS30 = 760 m/s, a.k.a. engineering rock). These scenarios were chosen because the magnitude range, strike-slip faulting mechanism and B/C reference site conditions are most common for hazard computations in California [29]. For this comparison, ASK14 is evaluated for default values of Z1.0 (= 0.0481 km) and ZTOR (= 6 km for M5, 3 km for M6, 1km for M7 and 0 km for M8) and BSSA14 is evaluated for default value of δz1 (= 0); these values were adapted from Gregor et al. [14]. Region parameter is set to 1 for ASK14 and 0 for BSSA14 considering California. The GK15 is evaluated for regional Q0 of 150, which is an average for California [30-32].

Figure 1a and Figure 2a illustrate short distance saturation as a function of magnitude for three GMPEs. For PGA and SA at 0.2 s, GK15 produces similar or slightly lower median results as compared to ASK14 and BSSA14 at close distances (0 – 2 km). The GK15 produces higher median predictions because of the over-saturation (bump) between 2 and 15 km. The bump phenomenon (also called oversaturation) was recently demonstrated through modeling geometrical spreading and relative amplitudes of ground motions in eastern North America. The bump was attributed to radiation pattern effects combined with wave propagation through a one-dimensional layered earth model [33,34]. In the case of earthquakes, this bump can be a result of one or many factors, including the aforementioned radiation pattern, directivity and nonlinear behavior of soil in near source of a fault [e.g., low-velocity fault zone-guided waves [35]] and measuring distance as that closest to the rupture plane and not from the seismogenic (most energetic) part of the fault rupture.

To quantify the differences for a range of magnitudes and distances, Figure 1b presents the ratio between median predictions of GK15 with those of ASK14. The upper and lower bounds of the shaded areas indicate a factor of two difference. The median predictions of GK15 are generally similar to those of ASK14 within a factor of 1.5 for PGA and SA at 0.2 s up to ~30 km for M5, ~45 km for M6 and 150 km for M7 and M8. For these IMs, the difference becomes more than two only for M5 after 50 km and for M6 events after ~90 km. At 150 km, the difference in PGA is less than 2.5 for M6 and four for M5. For SA at 0.2 s, the difference at 150 km is three for M6 and more than four for M5. For SA at 1.0 and 3.0 s, the difference between the GK15 median predictions and those of ASK14 are in general within a factor of 2.5 except for M5 beyond 40 km for SA at 1.0 s and ~75 km for SA at 3.0 s. At 150 km, the largest difference for M5 becomes 3.7 for SA at 1.0 s and 2.7 for SA at 3.0 s.

Figure 2b shows the ratios between the GK15 and BSSA14 median predictions. For PGA and SA at 0.2 s, the difference is within a factor of 1.5 for M6, 7 and 8 up to 150 km. For SA at 1.0 and 3.0 s, this difference is within a factor of two. The main difference between the GK15 and BSSA14 predictions is for M5 for SA at 1.0 and 3.0 s, which is within a factor of 3.5.

According to Gregor et al. [14], the median ground motions from NGA-West2 GMPEs are in general similar, within a factor of about 1.5¬–2 for 5 < M < 7 and distances between 10–100 km. We also performed similar comparisons in Figure 3, which demonstrates the median predictions between ASK14 and BSSA14, and their ratios. Although this figure elucidates that the difference between the GMPEs is generally in the range of 1.5¬–2, it is over 2 for M5 for SA at 1.0 and 3.0 s. For M5 and SA at 3.0 s, the difference becomes larger than 3.5 at short distances. The differences demonstrated in Figures 1b and 2b for GK15 are overall in agreement with the range of differences between ASK14 and BSSA14 shown in Figure 3.

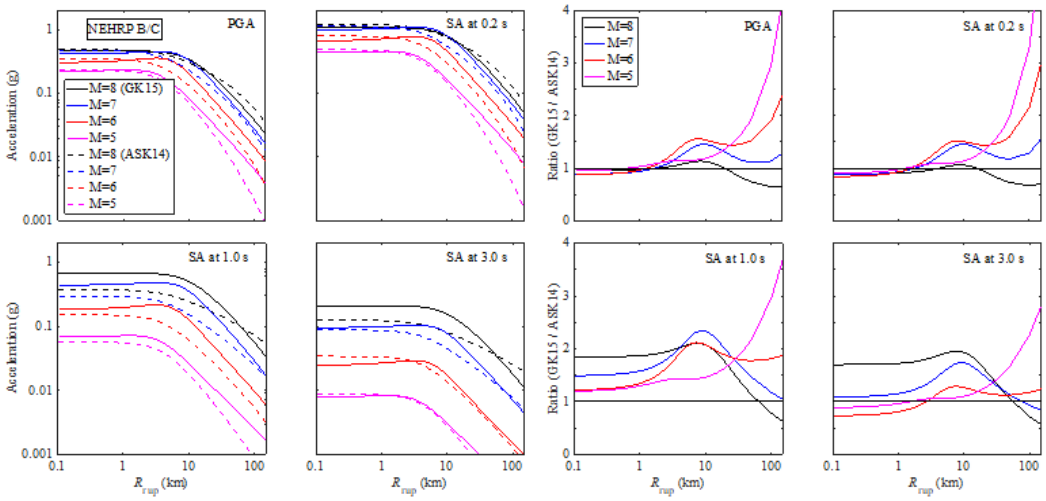

Figure 1(a): Comparison of distance-scaling (attenuation) features of median estimates of peak ground acceleration (PGA) and spectral accelerations (SA) at 0.2, 1.0 and 3.0 s predicted by the Graizer–Kalkan (2015; GK15) ground-motion prediction equation (GMPE) and the GMPE of Abrahamson et al. (2014; ASK14) for strike-slip moment magnitude (M) 5, 6, 7 and 8 earthquakes. VS30 = 760 m/s, Q0 = 150 and Bdepth = 0 km. Q0 and Bdepth are only used in GK15. Region is California. (Rrup = closest distance to fault rupture; VS30 = shear-wave velocity in the upper 30 m of the geological profile; Q0 = quality factor; Bdepth = depth to basin). (b) Ratio of median estimates between GK15 and ASK14; the upper and lower bounds of shaded areas indicate a factor of two difference.

Magnitude-Scaling Features

The effect of magnitude scaling for vertical strike-slip earthquakes at distances of 10, 30 and 150 km is shown in Figure 4 for VS30 = 760 m/s for median predictions of PGA and SA at 0.2, 1.0 and 3.0 s by the three GMPEs. ASK14 and BSSA14 were evaluated for default values as described previously. The magnitude range is taken from 5 to 8. Note that the break in the magnitude scaling of GK15 at M5.5 is driven by spectral shape of records used for constraining the magnitude-scaling function. The weak scaling of the short-period motion at short distances reflects the saturation with magnitude, common to all three GMPEs. The magnitude scaling features of these GMPEs show similarities and differences depending upon the intensity measure and magnitude level. For instance, the median ground motions are within a factor of two for short periods (PGA and 0.2 s) for M6 and above. At long periods, the range increases to a factor of 3 at M6 and above.

The differences between model predictions are larger for M5 espe-

cially at 150 km. We attributed such dissimilarities to regional variations and data used in constraining the GMPEs. In case of GK15, 97.9% of small magnitude (4.9 M < 6) earthquake data were from California (see Table 2 of Kalkan et al. [16] and the rest 3.1% were from Nevada, Italy and Taiwan. Whereas the ASK14 and BSSA14 G Spudich MPEs used small magnitude event data from other regions in larger percentages. Recent studies have shown that small-to-moderate magnitudes have different attenuation trends compared with the moderate-to-large magnitudes [36,37] and the regional variation is even more significant for smaller magnitudes [38].

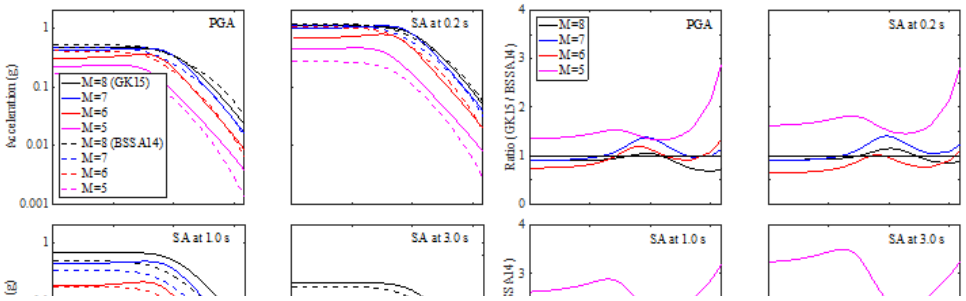

Figure 2(a): Comparison of distance-scaling (attenuation) features of median estimates of PGA and SA at 0.2, 1.0 and 3.0 s predicted by the GK15 GMPE and the GMPE of BSSA14 for strike-slip M5, 6, 7 and 8 earthquakes. RJB = Joyner-Boore distance. Region is California. All other parameters are defined in caption to Figure 1(b) Ratio of median estimates between GK15 and BSSA14; the upper and lower bounds of shaded areas indicate a factor of two difference.

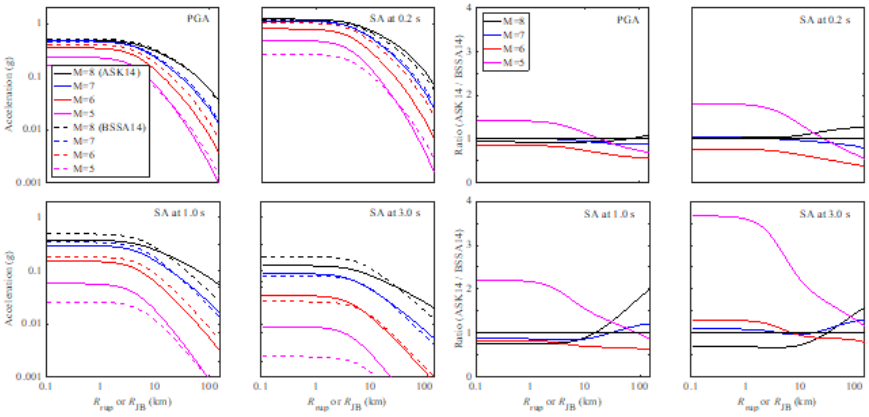

Figure 3(a): Comparison of distance-scaling (attenuation) features of median estimates of PGA and SA at 0.2, 1.0 and 3.0 s predicted by the ASK14 GMPE and the GMPE of BSSA14 for strike-slip M5, 6, 7 and 8 earthquakes. RJB = Joyner-Boore distance. Region is California. All other parameters are defined in caption to Figures 1 & 2(b) Ratio of median estimates between ASK14 and BSSA14; the upper and lower bounds of shaded areas indicate a factor of two difference.

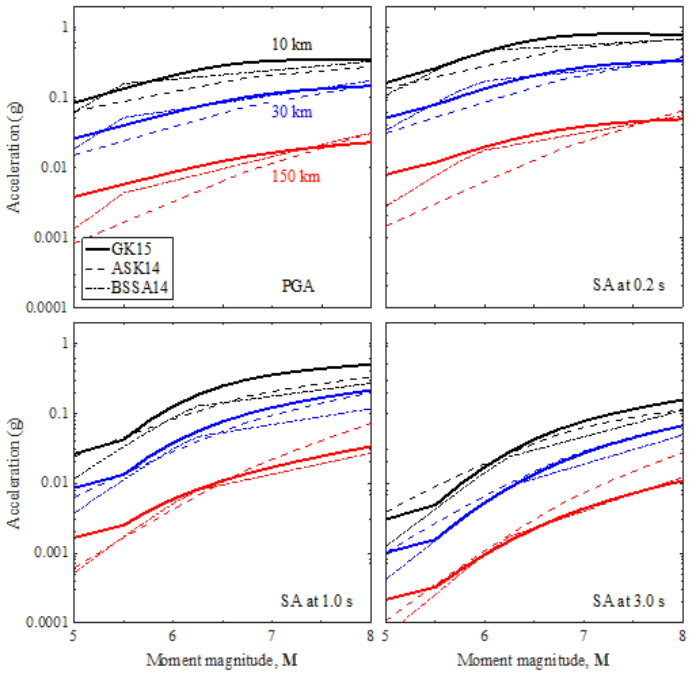

Figure 4: Comparison of magnitude-scaling features of median estimates of PGA and SA at 0.2, 1.0 and 3.0 s by the GK15 GMPE and the GMPEs of ASK14 and BSSA14 for 10, 30 and 150 km. Region is California. All other parameters are defined in caption to Figure 1.

Site Effects

All three GMPEs use VS30 for modeling site response scaling. A comparison of median spectrum as a function of VS30 values is shown in Figure 5 for a M7 vertical strike-slip earthquake at a closest distance of 10 and 50 km. For ASK14, ZTOR is taken as 1 km and for other parameters including Z1.0 and Z2.5 default values of ASK14 and BSSA14 are used. The GK15 is limited to VS30 ≥ 200 m/s and does not contain a nonlinear site amplification term because of the large variability in nonlinear site-correction models.

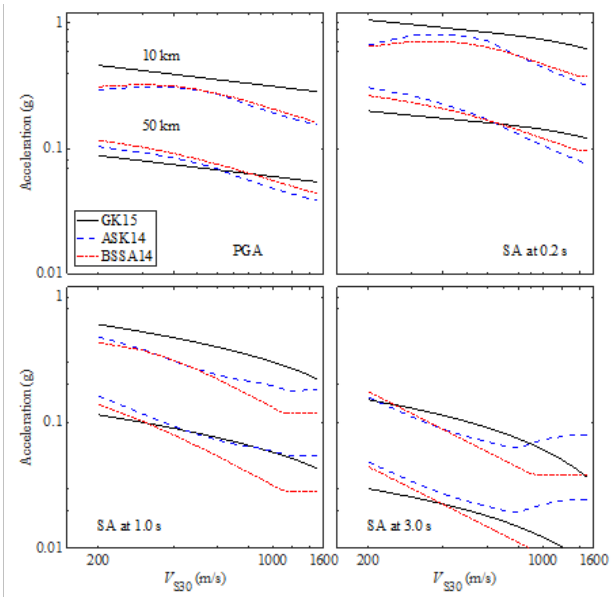

Figure 5: Comparison of VS30-scaling features of the median estimates of PGA and SA at 0.2, 1.0 and 3.0 s by the GK15 GMPE and the GMPEs of ASK14 and BSSA14 for a M7 strike-slip earthquake at 10 and 50 km. Region is California. All other parameters are defined in caption to Figure 1.

For higher VS30 values, ASK14 and BSSA14 saturate by predicting constant ground motion values. For shorter-distance (10 km), the nonlinear effects are apparent by the observed curvature in the amplification functions for ASK14 and BSSA14 especially for PGA and SA at 0.2 s. Overall, the site amplification results are alike among the three GMPEs; the largest difference is 35% between GK15 and other two GMPEs at 200 m/s for SA at 0.2 s.

Style-of-Faulting Effects

Figure 6 compares SOF ratios between reverse and strike-slip events and between normal and strike-slip events over the period range of 0.01 to 5 s at 30 km. These ratios are computed for a M7 event. In GK15, SOF factor is period and magnitude independent. In ASK14, magnitude-dependent but period-independent SOF factor was utilized for reverse and normal earthquakes only. In BSSA14, magnitude-dependent SOF factor, which is a function of period-dependent "hinge magnitude", was used for unspecified (U), strike-slip (SS), reverse (REV) and normal (NM) faults. GK15 predicts larger REV/SS ratios than either ASK14 or BSSA14. For REV/SS, the difference between ASK14 and BSSA14 are less than 10%, except at long periods. For NM/SS, the difference between two GMPEs are larger for short periods and gets similar at long periods. These comparisons suggest that there is a noteworthy variation [39-43].

Response Spectra

The linear site-effects scaling features between GK15 GMPE and two NGA-West2 GMPEs are compared in Figure 7 for a M7 strike-slip event at a distance of 30 km for a range of VS30 values representing NEHRP soil classifications B (VS30 = 750 and 1200 m/s), C (VS30 = 450 to 750 m/s) and D (VS30 = 250 to 450 m/s). The independent estimation parameters used in Figure 1 were repeated.

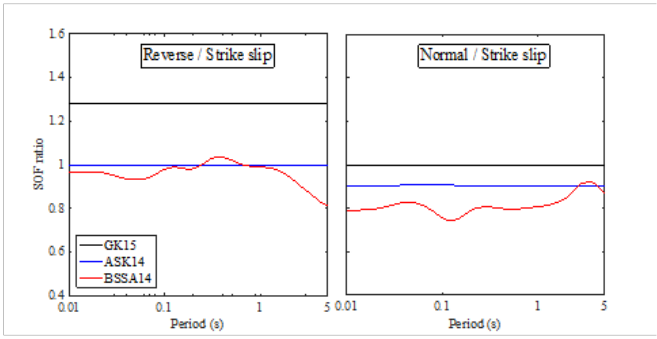

Figure 6: Comparison of style-of-faulting (SOF) ratios between reverse and strike-slip events and between normal and strike-slip events at 30 km among GK15, ASK14 and BSSA14.

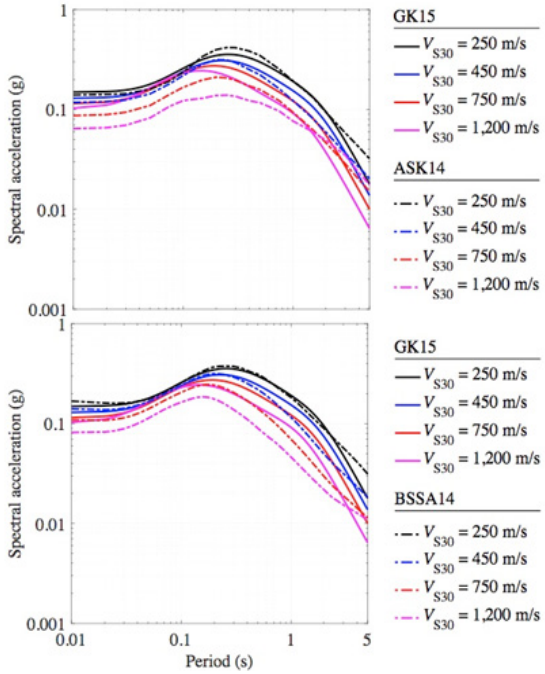

Figure 7: Comparison of VS30-scaling features of the median estimates of response-spectral shapes and amplitudes among GK15, ASK14 and BSSA14 for a strike-slip M7 earthquake at 30 km. All other parameters are defined in caption to Figure 1.

The spectral shapes from three GMPEs are similar between 0.01 and 3.0 s. The GK15 shows faster decay at long periods (3.0 to 5.0 s), controlled by the decay term in spectral shape prediction model, which is a function of basin depth. As compared to the two NGA-West2 GMPEs, variations in site-effects due to different site classes are less pronounced in the case of GK15 but the overall spectral shapes are analogous.

The median response spectra predicted by GK15 for M6, 7 and 8 earthquakes at 1 and 30 km from a vertically dipping strike-slip fault and VS30 = 760 and 270 m/s are compared with those predicted by ASK14 and BSSA14 in Figure 8 & Figure 9, respectively. Again, the same default parameters used in Figure 1 were repeated. There is resemblance (within a factor of 1.5) among the three models for the M6–8 cases. The difference between GK15 and ASK14 increases to a factor of two for the M8 case, especially at 1.0 s for VS30 = 760 m/s; this difference is much less for VS30 = 270 m/s. The largest relative change in the response spectra between GK15 and BSSA14 is for the long periods. For intermediate and short periods, the range in GK15 predictions is similar to BSSA14. For the M6 case, the response spectra predictions are generally close between the two GMPEs except for VS30 = 270 m/s at 30 km, where the differences are noticeably for a wide range of periods.

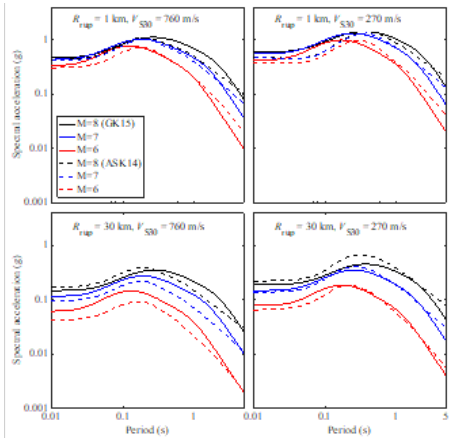

Figure 8: Comparison of the median estimates of response-spectral shapes and amplitudes between GK15 and ASK14 for strike-slip M6, 7 and 8 earthquakes at 1 and 30 km, VS30 = 270 and 760 m/s. All other parameters are defined in caption to Figure 1.

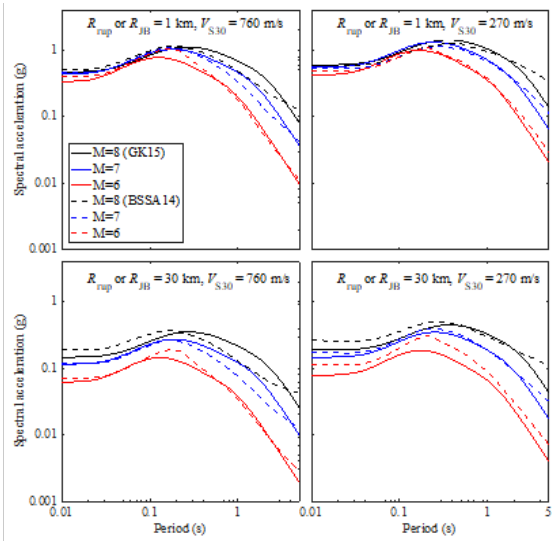

Figure 9: Comparison of the median estimates of response-spectral shapes and amplitudes between GK15 and BSSA14 for strike-slip M6, 7 and 8 earthquakes at 1 and 30 km, VS30 = 270 and 760 m/s. All other parameters are defined in caption to Figure 1.

Standard Deviations

Figure 10 compares the period-dependence of the standard deviations among GK15, σ ASK14 and BSSA14 for a M5 vertical strike-slip event at 30 km and VS30 = 760 m/s. All standard deviations (σ) are in natural logarithm units. Only the standard deviations of ASK14 are magnitude dependent. GK15 standard deviations are generally lower between 0.01 and 0.7 s. At 1.0 s, σ is similar between the three GMPEs. For longer spectral periods (> 1.0 s), GK15 has larger σ than the other two GMPEs. Differences are bigger for intra-event standard deviations (Ø than inter-event standard deviations (τ). Large Ø values for ASK14 and BSSA14 echo potential supplementary variability in PGA and SA due to additional events in NGA-West2 database. The ASK14 shows relatively flat τ trends with period, whereas the trends of τ for GK15 and BSSA14 are similar and fluctuate with period. The GK15 has lower values of Ø than the other GMPEs up to 0.7 s with the overall impact being the lowest vales of σ.

Stage 2: Comparisons with earthquake data: In Figure 11 & Figure 12 through Figure 13, SA predictions between 0.01 and 5 s from the three GMPEs are compared with the response spectra for near-field (0 to 20 km) and intermediate-field (50 to 70 km) ground-motion records of select major earthquakes in California from the NGA-West2 database. Specifically, the 1966 M6.2 Parkfield, 1979 M6.5 Imperial Valley, 1984 M6.2 Morgan Hill, 1986 M6.1 N. Palm Springs, 1987 M6.5 Superstition Hills, 1989 M6.9 Loma Prieta, 1992 M7.3 Landers, 1994 M6.7 Northridge, 2004 M6 Parkfield and 2010 M7.2 El-Mayor Cucapah earthquakes are covered. Among all the events listed, the M7.2 El-Mayor Cucapah is not in the GK15 database. Our objective here is to demonstrate the performance of the GMPEs in predicting the ground motions from California regardless of whether the particular event was used in deriving the GMPE.

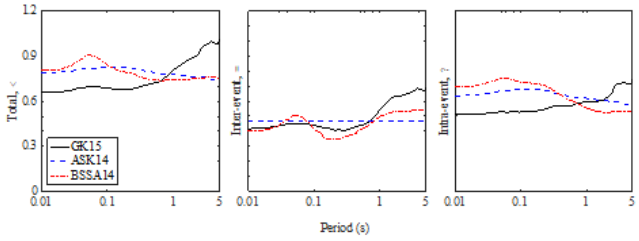

Figure 10: Comparison of total, inter-event and intra-event variability of the GK15 GMPE with the GMPEs of ASK14 and BSSA14 for a M5 earthquake.

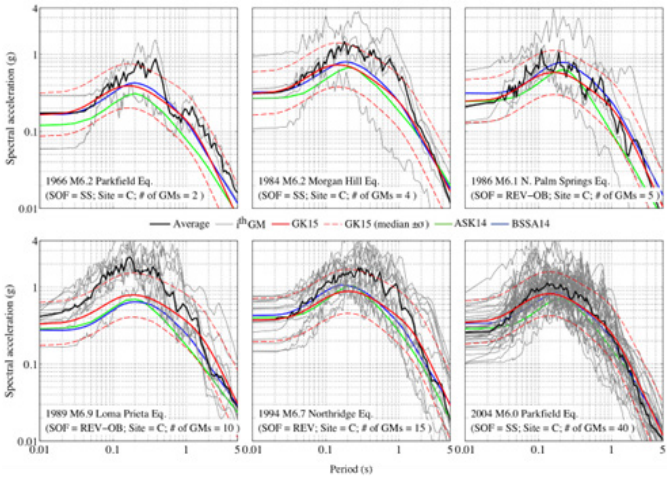

Figure 11: Comparison of the median estimates of response-spectral shapes and amplitudes by the GK15 GMPE and the GMPEs of ASK14 and BSSA14 with the observations from select six major Californian earthquakes from the NGA-West 2 database. Ground-motion data correspond to near-field records (0 – 20 km) with NEHRP site class C. Dash curves indicate 16th and 84th percentile predictions by the GK15. SOF = style of faulting; SS = strike-slip; REV = reverse; REV–OB: Reverse oblique). Number of ground motions (GMs) from each earthquake are indicated.

In these figures, the ground-motion records correspond to NEHRP site classification C or D. The number of records satisfying the distance and soil condition selection criteria is listed on each panel where the average spectra of records are shown by thick jagged curves and they are compared with the predictions. Individual spectra of records are also shown by thin jagged curves to demonstrate the variability. The predictions are for the average VS30 of each ground-motion set. The 16th and 84th percentile predictions of GK15, shown by dashed curves, bound the majority of the SA data. For all events in near- and intermediate-field, the GK15 yields predictions closer to the average of the observations [predicted and observed trends of the peak (period and amplitude) of the response spectra with magnitude and distance match]. The width of the predicted response spectra is also comparable to the observations. Some of the variability is possibly due to the fluctuations of the site condition within the site class. The predictive response spectra by GK15 are also close to those estimated by the other two GMPEs.

The comparisons considering the strong-motion data of the 2014 M6 South Napa earthquake—the most recent damaging event in California—yielded similar results as shown in Kalkan et al. [16].

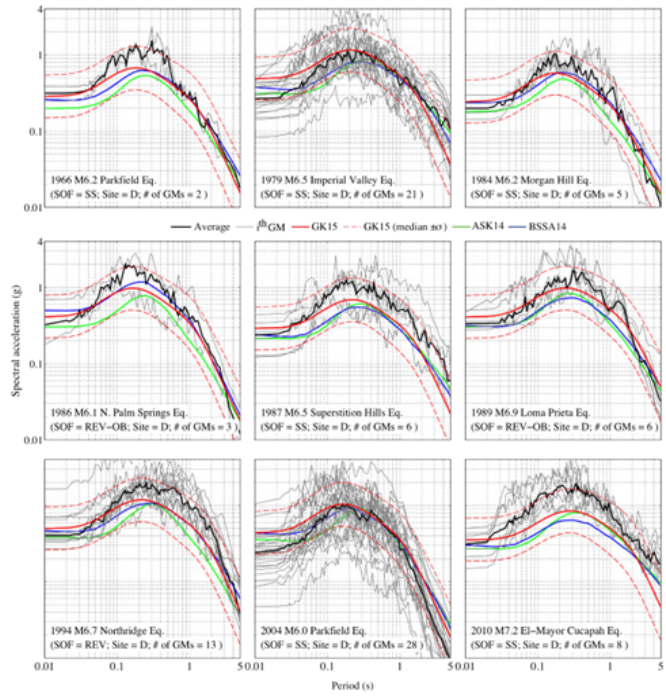

Figure 12: Comparison of the median estimates of response-spectral shapes and amplitudes by the GK15 GMPE and the GMPEs of ASK14 and BSSA14 with the observations from select nine major Californian earthquakes from the NGA-West 2 database. Ground motion data correspond to near-field records (0 – 20 km) with NEHRP site class D. Dash curves indicate 16th and 84th percentile predictions by the GK15.

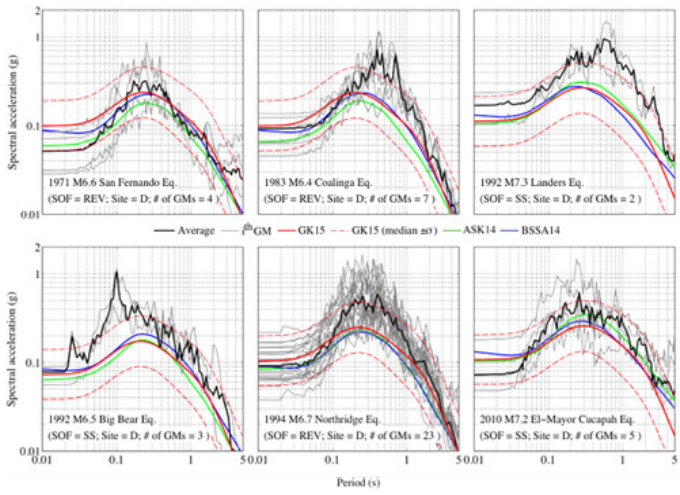

Figure 13: Comparison of the median estimates of response-spectral shapes and amplitudes by GK15, ASK14 and BSSA14 with the observations from select six major Californian earthquakes from the NGA-West 2 database. Ground motion data correspond to intermediate-field records (50 – 70 km) with NEHRP site class D. Dash curves indicate 16th and 84th percentile predictions by the GK15.

Stage 3: Comparisons of residuals using NGA-West2 database: We performed mixed-effects residuals analyses in order to evaluate how well GK15, ASK14 and BSSA14 predict the near-source (within 80 km of the fault) subset of the NGA-West2 database and to confirm that GK15 is not biased with respect to M, Rrup, VS30, Bdepth and style-of-faulting (F) parameters by examining trends of residuals against them. The dataset covers 975 ground-motion data from 73 Californian events ranging from M5 to 7.36. The analysis results reveal that the GK15 is generally unbiased with respect to its independent predictors including moment magnitude, closest distance to fault, VS30, style-of-faulting and basin depth. Due to space limitation, the residual analyses results are shown in Kalkan et al. [16].

Table 1 compares the standard deviations of residuals among three GMPEs considering the near-source California subset of the NGA-West2 database. The values in natural logarithm units are computed for four IMs. The terms of standard deviations including intra-event, inter-event and total are very similar among the three GMPEs, and their values increase with spectral period. These results underline that the GK15 does not always have the lowest standard deviations.

Conclusion

We compared systematically the GMPE of Graizer-Kalkan [1,2] with the NGA-West2 GMPEs of Abrahamson et al. [3] and Boore et al. [4] to evaluate the similarities and differences among them. The key findings of this study are as follows:

1. GK15 GMPE and the other two NGA-West2 GMPEs demonstrate median ground-motion estimates for California generally within a factor of 1.5¬–2 for magnitudes between 5 and 7. The largest differences are for very large magnitudes with no or sparse data or for small magnitudes at long distances. To account for the variability density of data in different magnitude and distance bins, Petersen et al. [29] introduced additional epistemic uncertainty terms for hazard computations.

2. GK15 produces similar or slightly smaller ground motions at very close distances to the fault (up to about 5 km) and at distances of more than 20 km from the fault for earthquakes with magnitude larger than 6. Between 5 and 20 km, GK15 results in higher estimates of ground motion than either ASK14 or BSSA14 does. The distance scaling of the GMPEs shows some differences, which stem from different functional forms used for distance scaling and dataset used for constraining the estimation coefficients of each GMPE.

3. An additional difference between the GK15 and other two GMPEs that was not directly assessed in the comparisons, but is essential, is related to the inclusion of quality factor (Q0). The GK15's use of Q0 that can be changed to suit the region of interest is an improvement over other GMPEs. On the other hand, GK15 neither includes nonlinear-site response nor hanging wall effect.

4. The standard deviations of original GMPEs are different. At short periods up to 0.7 s, GK15 offers lower standard deviations than the ASK14 and BSSA14 GMPEs do. At longer periods (over 1.0 s), standard deviations of other GMPEs are lower than those of the GK15. When the subset of the NGA-West2 database is considered, the terms of standard deviations (total, intra- and inter-event) among three GMPEs become similar; for instance, total standard deviation for three GMPEs is between 0.65 and 0.69 for PGA, 0.7 and 0.76 for SA at 0.2 s, 0.89 and 1.07 for SA at 1.0 s, and 1.07 and 1.42 for SA at 3.0 s.

References

1. Graizer V, Kalkan E (2015) Update of the Graizer-Kalkan Ground-Motion Prediction Equations for Shallow Crustal Continental Earthquakes. U.S. Geological Survey Open-File Report 2015-1009, pp: 1-98. .

2. Graizer V, Kalkan E (2016) Summary of GK15 Ground-Motion Prediction Equation for Predicting PGA and 5%-damped SA from Shallow Crustal Continental Earthquakes. Bull of Seism Soc of Am 106(2): 687-707.

3. Abrahamson NA, Silva WJ, Kamai R (2014) Summary of the ASK14 Ground Motion Relation for Active Crustal Regions. Earthquake Spectra 30(3): 1025-1055.

4. Boore DM, Watson-Lamprey J, Abrahamson NA (2006) Orientation-independent measures of ground motion. Bull Seism Soc Am 96(4A): 1502-1511.
5. Chiou B, Darragh R, Gregor N, Silva W (2008) NGA project strong-motion database. Earthquake Spectra 24(1): 23-44.
6. Graizer V, Kalkan E (2007) Ground-motion attenuation model for peak horizontal acceleration from shallow crustal earthquakes. Earthquake Spectra 23(3): 585-613.
7. Graizer V, Kalkan E (2009) Prediction of response spectral acceleration ordinates based on PGA attenuation. Earthquake Spectra 25(1): 39-69.
8. Bozorgnia Y, Abrahamson NA, Al Atik L, Ancheta TD, Atkinson GM, et al. (2014) NGA-West2 research project. Earthquake Spectra 30(3): 973-987.
9. Baltay AS, Boatwright J (2015) Ground-motion observations of the 2014 South Napa earthquake. Seismological Research Letters 86(2A): 355-360.
10. Boore MD, Stewart JP, Seyhan E, Atkinson GM (2014) NGA-West2 Equations for Predicting PGA, PGV, and 5% Damped PSA for Shallow Crustal Earthquakes. Earthquake Spectra 30(3): 1057-1085.
11. Campbell KW, Bozorgnia Y (2014) NGA-West2 Ground Motion Model for the Average Horizontal Components of PGA, PGV, and 5%-Damped Linear Acceleration Response Spectra. Earthquake Spectra 30(3): 1087-1115.
12. Chiou B, Youngs RR (2014) Update of the Chiou and Youngs NGA Model for the Average Horizontal Component of Peak Ground Motion and Response Spectra. Earthquake Spectra 30(3): 1117-1153.
13. Idriss IM (2014) An NGA-West2 Empirical Model for Estimating the Horizontal Spectral Values Generated by Shallow Crustal Earthquakes. Earthquake Spectra 30(3): 1155-1177.
14. Gregor N, Abrahamson NA, Atkinson GM, Boore DM, Bozorgnia Y, et al. (2014) Comparison of NGA-West2 GMPEs. Earthquake Spectra 30(3): 1179-1197.
15. Campbell KW (2016) Comprehensive Comparison among the Campbell–Bozorgnia NGA-West2 GMPE and Three GMPEs from Europe and the Middle East. Bull Seismol Soc Am 106(5): 2081-2103.
16. Kalkan E, Graizer V (2019) Comparison of the Graizer-Kalkan (GK15) GMPE with Two NGA-West2 GMPEs for California. U.S. Geological Survey Open-File Report (in-press).
17. Ancheta TD, Darragh RB, Stewart JP, Seyhan E, Silva WJ, et al. (2014) NGA-West2 database. Earthquake Spectra 30(3): 989-1005.
18. Mak S, Clements RA, Schorlemmer D (2017) Empirical evaluation of hierarchical ground-motion models: Score uncertainty and model weighting. Bull Seismol Soc Am 107(2): 949-965.
19. Van Houtte C, Bannister C, Holden C, Bourguignon S, Mc Verry G (2017) The New Zealand strong motion database. Bull New Zeal Soc Earthq Eng 50(1): 1-20.
20. Farhadi A, Pezeshk S, Khoshnevis N (2018) Assessing the Applicability of Ground-Motion Models for Induced Seismicity Application in Central and Eastern North America. Bull Seismol Soc Am 108(4): 2265-2277.
21. Baker JW, Jayaram N (2008) Correlation of spectral acceleration values from NGA ground motion models. Earthquake Spectra 24(1): 299-317.
22. Thorburn WM (1915) Occam's razor. Mind 24: 287-288.
23. Cairns AJG (2000) A Discussion of Parameter and Model Uncertainty in Insurance. Insurance: Mathematics and Economics 27(3): 313-330.
24. Jeffreys H (1961) Theory of Probability. 3rd (Edn.), Oxford University Press, Oxford.
25. Vandekerckhove J, Matzke D, Wagenmakers EJ (2015) Model comparison and the principle of parsimony. In Busemeyer J, Townsend J, Wang ZJ, Eidels A (Eds.), Oxford handbook of computational and mathematical psychology, Oxford, UK: Oxford University Press, pp: 1-21.
26. Sadigh K, Chang CY, Egan JA, Makdisi F, Youngs RR (1997) Attenuation relationships for shallow crustal earthquakes based on California strong motion data. Seismological Research Letters 68(1): 180-189.
27. Kamai R, Abrahamson NA, Silva WJ (2014) Nonlinear horizontal site amplification for constraining the NGA-West2 GMPEs. Earthquake Spectra 30(3): 1223-1240.
28. Seyhan E, Stewart JP (2014) Semi-empirical nonlinear site amplification from NGA-West 2 data and simulations. Earthquake Spectra 30(3): 1241-1256.
29. Petersen MD, Moschetti MP, Powers PM, Mueller CS, Haller KM, et al. (2014) Documentation for the 2014 update of the United States national seismic hazard maps. U.S. Geological Survey Open-File Report 2014–1091, pp: 243.
30. Singh S, Herrmann RB (1983) Regionalization of crustal coda Q in the continental United States. J Geophys Res 88(B1): 527-538.
31. Mitchell BJ, Hwang HJ (1987) Effect of low Q sediments and Crustal Q on Lg attenuation in the United States. Bull Seismol Soc Am 77(4): 1197-1210.
32. Erickson D, McNamara DE, Benz HM (2004) Frequency dependent Lg Q within the continental United States. Bull Seismol Soc Am 94(5): 1630-1643.
33. Chapman MC, Godbee RW (2012) Modeling geometrical spreading and the relative amplitudes of vertical and horizontal high-frequency ground motions in eastern North America. Bull Seism Soc Am 102(5): 1957-1975.
34. Baumann C, Dalguer LA (2014) Evaluating the compatibility of dynamic rupture-based synthetic ground motion with empirical ground-motion prediction equation. Bull Seism Soc Am 104(2): 634-652.
35. Li YG, Vidale JE (1996) Low-velocity fault-zone guided waves: Numerical investigations of trapping efficiency. Bull Seism Soc Am 86(2): 371-378.
36. Chiou B, Youngs R, Abrahamson N, Addo K (2010) Ground-motion attenuation model for small-to-moderate shallow crustal earthquakes in California and its implications on regionalization of ground-motion prediction models. Earthq Spectra 26(4): 907-926.
37. Atkinson GM, Morrison M (2009) Observations on regional variability in ground-motion amplitudes for small-to-moderate earthquakes in North America. Bull Seismol Soc Am 99(4): 2393-2409.
38. Zafarani H, Farhadi A (2017) Testing ground-motion prediction equations against small-to- moderate magnitude data in Iran. Bull Seismol Soc Am 107(2): 912-933.
39. Al Atik L, Youngs RR (2014) Epistemic uncertainty of NGA West 2 models. Earthquake Spectra 30(3): 989-1005.
40. Douglas J, Jousset P (2011) Modeling the Difference in Ground-Motion Magnitude-Scaling in Small and Large Earthquakes. Seismological Research Letters 82(4): 504-508.
41. Ford SR, Dreger DS, Mayeda K, Walter WR, Malagnini L, et al. (2008) Regional attenuation in northern California: A comparison of five 1D Q methods. Bull Seismol Soc Am 98(4): 2033-2046.
42. Joyner WB, Boore DM (1993) Methods for regression analysis of strong-motion data. Bull Seism Soc Am 83(2): 469-487.
43. Spudich P, Joyner WB, Lindh AG, Boore DM, Margaris BM, et al. (1999) SEA99: a revised ground motion prediction relation for use in extensional tectonic regimes. Bull Seism Soc Am 89(5): 1156-1170.